Received: 26 November 2017 | Revised: 31 July 2018 | Accepted: 2 September 2018

DOI: 10.1002/tal.1554

RESEARCH ARTICLE

WILEY

Energy dissipation and performance assessment of double damped outriggers in tall buildings under strong earthquakes

Mauricio Morales-Beltran[1,2] | Gürsoy Turan[3] | Onur Dursun[2] | Rob Nijsse[1]

[1] Faculty of Architecture and the Built Environment, TU, Delft, the Netherlands

[2] Department of Architecture, Yaşar University Izmir, Bornova, Turkey

[3] Department of Civil Engineering, Izmir Institute of Technology IYTE, Urla, Turkey

Correspondence
Mauricio Morales-Beltran, Faculty of Architecture and the Built Environment, TU, Delft, the Netherlands.
Email: m.g.moralesbeltran@tudelft.nl; mauricio.morales-beltran@yasar.edu.tr

Present Address
Mauricio Morales-Beltran, Faculty of Architecture, Yaşar University, Universite Caddesi, No. 35–37, Bornova 35100, İzmir, Turkey.

Funding information
Fondo de Fomento al Desarrollo Científico y Tecnológico, Grant/Award Number: 72100284

Summary

The use of a single set of outriggers equipped with oil viscous dampers increases the damping ratio of tall buildings in about 6–10%, depending on the loading conditions. However, could this ratio be further increased by the addition of another set of outriggers? Should this additional set include dampers too? To answer these questions, several double damped outrigger configurations for tall buildings are investigated and compared with an optimally designed single damped outrigger, located at elevation 0.7 of the total building's height (h). Using free vibration, double outrigger configurations increasing damping up to a ratio equal to the single-based optimal are identified. Next, selected configurations are subjected to several levels of eight ground motions to compare their capability for avoiding damage under critical excitations. Last, a simplified economic analysis highlights the advantages of each optimal configuration in terms of cost savings. The results show that, within the boundaries of this study, combining a damped outrigger at 0.5h with a conventional outrigger at 0.7h is more effective in reducing hysteretic energy ratios and economically viable if compared with a single damped outrigger solution. Moreover, double damped outrigger configurations for tall buildings exhibit broader display of optimal combinations, which offer flexibility of design to the high-rise architecture.

KEYWORDS

cost savings, damped outrigger, energy dissipation, strong earthquakes, tall buildings, viscous damper

1 | INTRODUCTION

Outrigger systems consist of a series of cantilever truss beams or shear walls connecting the building core with the perimeter columns. As result, the axial forces acting at the end of the outriggers help the reduction of the total deflection of tall buildings, by increasing the restoring moment. Dampers have been introduced between the perimeter columns and the outriggers resulting in an increase in the overall damping of the building.[1] A few implementations of this system, called damped outrigger, have been reported elsewhere.[2–4] Both practice and research have shown that an optimal outrigger location and damping coefficient of the dampers largely influence the increase of the damping ratio.[1,3–8] Under an optimal configuration, damped outriggers are meant to absorb the excessive earthquake energy that would otherwise cause damage in the structure. Nevertheless, under large or severe earthquake-induced motion, some plastic hinges or failures may be produced in the host structure before the dampers are able to dissipate the total input energy.

Despite the need of an assessment of the building response by which the damage potential can be quantified, most of the extensive studies on damped outriggers for seismic control of tall buildings focus on the reduction of the response in terms of peak values.[5,6,8–11] Only few studies consider the combined influence of the intensity, frequency content, and duration of these large earthquakes in the control performance of the damped outriggers. Energy-based design methods have the potential to address both the effect of the duration of the earthquakes and the hysteretic behaviour of structure.[12] As addressed by Uang and Bertero,[13] an energy-based design method is based on the premise that the energy demand during an earthquake can be predicted as the energy supplied by the structure can be therefore defined. Consequently, a correct design implies that the energy supply is larger than the energy demand. On the other hand, the application of damped outriggers for reducing the building's seismic response lies on the assumption that dampers will absorb the total earthquake energy, as the rest of the structure remains elastic during the seismic event. Nevertheless, under large or severe earthquake-induced motion, some plastic hinges or failures may be produced in the structure before the dampers are able to dissipate the total input energy. Hysteretic behaviour of the host structure, then, needs to be evaluated along the dampers' performance in order to determine how the earthquake input energy is distributed through all the components.

This article provides an analytical framework to comparatively assess the distribution of seismic energy in tall buildings equipped with viscous damped outriggers, that is, with outriggers that have one or more viscous damper installed between their ends and the perimeter columns. Because previous research developed by the authors showed that the energy dissipation capacity of a single set of outrigger will not prevent damage under strong earthquakes,[14] a subsequent question was whether adding another set of outriggers would enhance such performance. In other words, if a single damped outrigger structure is designed to reach an optimal damping ratio, could this damping ratio still be increased by the addition of another set of outriggers? Should this additional set of outriggers be equipped with dampers too? In order to investigate the benefit of an extra set of damped outriggers, a comparative study is presented, wherein several double set of outrigger configurations for tall buildings are investigated and compared with an optimally designed single damped outrigger, located at elevation 0.7 of the total building's height (h). First, using free vibration analyses, those double outrigger configurations increasing damping up to a ratio equal or larger than that of the optimal single outrigger are identified. Second, all these hereafter optimal configurations are subjected to small, moderate, strong, and severe earthquake levels of eight ground motions to critically compare the capability of such configurations for dissipating seismic energy and thus avoiding extended damage under critical excitations.

Finally, because practice has shown that with the addition of supplemental damping, construction costs are reduced,[4] a simplified economic analysis is applied to investigate possible advantages of each optimal configuration in terms of steel reinforcement savings versus damper cost, as a consequence of the reduction in overturning moment (OTM) and base shear. The results show that, within the boundaries of this study, combining a damped outrigger at 0.5h with a conventional outrigger at 0.7h is both more effective in reduce hysteretic energy ratios under strong earthquakes and economically viable if compared with a single damped outrigger solution.

2 | METHODOLOGY

2.1 | Analytical models and non-linear time-history analyses

The analytical models used in this study are based on the existing Shangri-La building in Manila, Philippines, as described in Willford and Smith.[4] Although the actual 60-storey Shangri-La building features wall-type or deep beam outriggers, a truss girder model for the outrigger configuration is proposed in this study as it enables a more efficient use of the space for functional purposes. The 2D models described here consider only two and four outriggers per side, each pair modelled as a single 7-m-high outrigger, as displayed in Figure 1. In the models, both building plan and

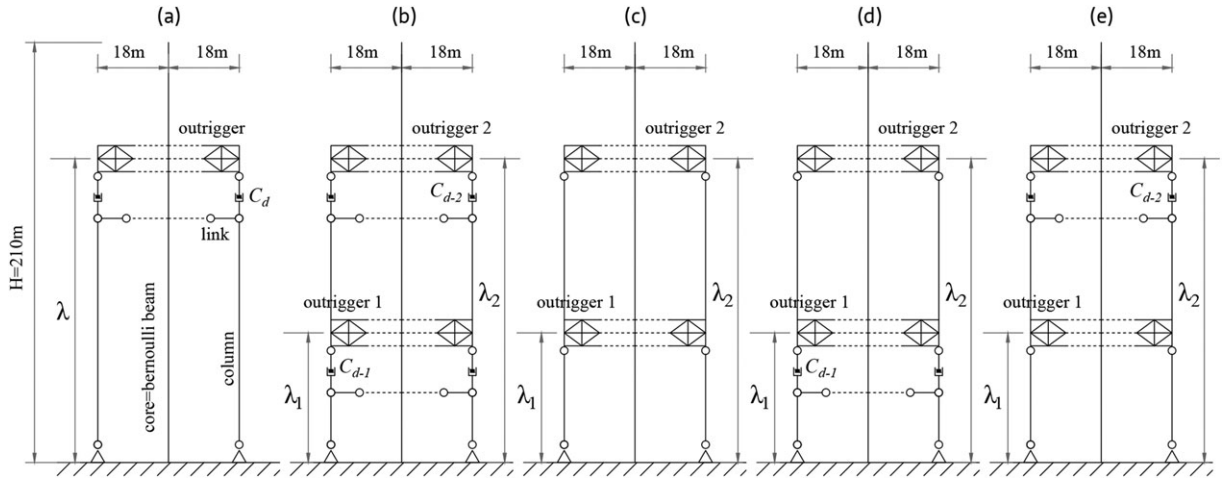

FIGURE 1 Analytical outrigger building models: (a) single damped, (b) double damped, (c) double fixed, (d) combined damped and fixed, and (e) combined fixed and damped

distribution of resistant elements are symmetrical so the lateral stiffness in two orthogonal directions is assumed equal. Nodal masses were added to account for the load of secondary structural components, such as slabs and steel frames. The core is an 18 m × 18 m reinforced concrete tube, with a constant thickness of 0.75 m. The finite element (FE) model of the core is modelled as a Bernoulli–Euler cantilever beam type that is dominated by bending deformation. The area of the reinforced concrete perimeter columns is 1.30 m^2.

Both core and outrigger were modelled using non-linear settings, as they are expected to be the major sources of hysteretic energy dissipation. The analytical model described here, therefore, considers the use of general non-linear material models throughout almost the whole FE model as specified by Diana-FEA software (2016).[15] The total strain crack model is used to define the non-linear behaviour of the concrete, based on a bi-linear stress–strain relationship as defined in Eurocode 2.[16] Both the influence of the lateral confinement and the lateral influence of cracking in the reduction of strength after cracking are considered. The reduction of the Poisson effect after cracking is also considered because such effect ceases to exist when the material cracks. Maximum longitudinal reinforcement was provided only over the lower section of the building (six floors) and decreased towards the upper levels. This distribution was defined following the capacity flexural strength design envelope as proposed by Boivin and Paultre,[17] with a minimum reinforcement[18] ratio = 0.25%. In the case of steel, the plasticity model of Von Mises and an ideal elasto-plastic model are considered for its constitutive behaviour, that is, strain hardening effect is not taken into account. This is considered as a post-yield reserve of ductility. Properties of the steel are derived from Eurocode 3.[19] More details on the non-linear settings of these FE models in Diana-FEA can be found elsewhere.[14]

Finally, because the dampers used in this study are velocity-dependant, the benefit of the increased damping they provided is only included when considering dynamic loading. Therefore, time-history response analysis in Diana-FEA is used for accounting the influence of the supplemental damping in the response reduction.

2.2 | Optimal increase of inherent damping ratio (ζ) through free vibration analyses

In order to set a valid comparative framework, all models present configurations that are optimal from the perspective of increasing the inherent damping ratio (ζ) of the bare structure, that is, 2%. Sensitivity analyses were conducted on several configurations where both outrigger locations (λ) and dampers' damping coefficient (C_d) were systematically modified in order to obtain significant increases of ζ. A logarithmic decrement technique, under free vibration, was used to determine such optimal ζ.

For simplicity, λ is defined as multiplicand of the total height H, ranging between 0.1 and 1.0 at intervals of 0.1. The variation of C_d, nonetheless, is less straightforward and requires performing sensitivity analyses before defining a range of feasible values. For example, in the case of a single damped outrigger, values smaller than 1.5E + 03 kN-s/m have no influence, and the building behaves as a cantilever beam, that is, without the contribution of the outriggers; values larger than 1.5E + 06 kN-s/m dynamically stiffen the damper, and the building behaves similarly to one equipped with conventional (or *undamped*) outriggers. Although the optimal value for a single damped outrigger is about 9.8E + 04 kN-s/m, the variation in the response does not linearly follow the variation at regular intervals, departing from this optimal C_d. It was found that a range between 2.4E + 04 and 6.72E + 5, using intervals of 7.2E + 04 kN-s/m, produces substantial variations in the building's response without incrementing the number of computational simulations. Evidently, this range is the same for all the studied models.

2.3 | Energy balance equations

The equation governing the dynamic response of a multi-degree of freedom, such as a tall building, can take the form

$$M_{\ddot{x}} + C_{\dot{x}} + K_x = -M\Gamma\ddot{x}_g, \tag{1}$$

where M and K are the diagonal lumped mass and stiffness matrices, respectively; C is the damping matrix computed considering Rayleigh damping; x is the column vector of relative displacements of the node mass with respect to ground; $\ddot{x}_g$ is the one-dimensional ground acceleration; and Γ is the influence vector that accounts for the effect of ground excitation on a specific degree of freedom of the structure. If Equation (1) is multiplied by the transpose of the relative velocity vector $\dot{x}_t$ and integrated over the entire duration of the ground motion (0-t), the equation of motion can be expressed in terms of the energy balance equation as follows:

$$\int_0^t \dot{x}^T M\ddot{x}dt + \int_0^t \dot{x}^T C\dot{x}dt + \int_0^t \dot{x}^T \Lambda C_d \dot{x}_d{}^\kappa dt + \int_0^t \dot{x}^T Kxdt = -\int_0^t \dot{x}^T M\Gamma\ddot{x}_g dt, \tag{2}$$

where Λ is the location matrix of the dampers, associated to the outrigger location λ; C_d is the damping coefficient of the viscous dampers; $\dot{x}_d$ is the velocity across the damper; and κ is the exponent value that controls the linear/non-linear behaviour of the damper. In this case, κ = 1.

All terms in Equation (2) can be written separately as

$$E_K = \int_0^t \dot{x}^T M\ddot{x}\, dt = \frac{1}{2}\dot{x}^T M\dot{x} \quad ; \quad E_D = \int_0^t \dot{x}^T C\dot{x}\, dt \quad ; \quad E_{\text{dampers}} = \int_0^t \dot{x}^T \Lambda C_d \dot{x}_d{}^\kappa\, dt \quad E_A = \int_0^t \dot{x}^T Kx\, dt \quad ; \quad E_I = -\int_0^t \dot{x}^T M\Gamma\ddot{x}_g\, dt, \tag{3}$$

where E_K, E_D, E_{dampers}, E_A, and E_I are the kinetic, (inherent) damping, dampers (supplemental damping), absorbed, and input energies, respectively. Moreover, because the structure absorbs energy by a combination of elastic and inelastic mechanisms, E_A can also be defined as

$$E_A = E_S + E_H \quad ; \quad E_S = \frac{1}{2}\dot{x}^T K x \quad ; \quad E_H = \int f_s\left(x - x_{\text{yield}}\right) dx + \int M_b\left(\theta - \theta_{\text{yield}}\right) d\theta, \tag{4}$$

where E_S and E_H are the elastic strain and hysteretic energies, respectively; f_s is the restoring force; M_b is the bending moment; and θ is the associated angle of rotation. Due to the assumption of a Bernoulli beam in the modelling of the core and the outrigger frame, stresses and strains derived from shear forces are not considered in the derivation of E_H.

Finally, replacing Equations (3) and (4) in Equation (2), the energy balance equation for a multi-degree-of-freedom system is given by

$$E_K + E_D + E_{\text{dampers}} + E_S + E_H = E_I. \tag{5}$$

Although the exponent κ in Equations (2)–(3) can be varied[3] between 0.15 and 2, in all the analysis in this study $\kappa = 1$, implying that the damping forces provided by the damper will be linearly proportional to the velocity. The use of $\kappa\sim = 2$ implies high forces at lower velocities, whereas the opposite occurs when lower values of κ are used. Under strong earthquake motions, the use of a lower exponent might lead to the insensitivity of the dampers to low velocities, whereas the use of a linear exponent might lead to excessive damping forces, if compared with the wind damping.[3] The reason for $\kappa = 1$ is that comparatively excessive damping forces may help understand the role of the outrigger's bending and shear stiffness in the distribution of seismic energy in the building structure. If, as a result of this assumption, the damping forces are indeed excessive, the use of a relief valve may help to avoid their negative effects over the outrigger structure.

2.4 | Assessment of the distribution of seismic energy in a tall building

In an energy-based design of buildings, the first five terms in Equation (5) considered the energy capacity of the structure, whereas the right-hand-side term considered the energy demand. From a seismic design perspective, it is obvious that the capacity of the structure should be larger than the response demand, that is, energy capacity > energy demand. For a non-linear system subjected to ground motions, strain and kinetic energies are relatively small, and at the end of the response, both E_K and E_S become zero. Hence, they are not affected by the duration of strong motion,[12] and it is valid to assume that, by the end of the motion, E_I is mostly defined by the combined effect of damping energies ($E_D + E_{\text{dampers}}$) and hysteretic energy (E_H) dissipation. On the other hand, maximum damping and hysteretic energies show the energy dissipation capacity that can be used to enhance the design and limit the structural damage. Therefore, insights on how these energies are related may be more significant for the assessment of the seismic energy distribution in the damped outriggers, than spotting single-based performances. These relationships can be expressed by (a) the ratio of hysteretic-to-input energy, defined as the hysteresis energy ratio E_H/E_I; (b) the ratio of damping-to-input energy, defined as the inherent viscous damping energy ratio E_D/E_I; and (c) the ratio of dampers-to-input energy, defined as the supplemental damping ratio E_{dampers}/E_I. Whereas $E_H/E_I = 1$ implies that the total change in input energy is dissipated by extended damage and/or failure of the structure, a value of zero implies no structural damage.[20] Furthermore, $E_H/E_I = 0$ implies elastic behaviour in all the elements of the structure, during the entire ground motion. Because this latter case is highly unlikely under strong and severe earthquake levels, the purpose of the following studies is to determine which outrigger configurations extend the threshold where energy dissipation due to hysteresis can be fully replaced by energy dissipated through the action of viscous dampers. Finally, in this study, all energies are computed using relative coordinates as the authors believe that the use of relative energy terms instead of absolute ones is more meaningful for engineering applications. For an extended discussion on the subject, the reader is referred to Morales-Beltran.[21]

2.5 | Earthquake levels

Eight earthquake records were used in the analysis. These records were scaled down/up based on peak ground velocity rather than on peak ground acceleration. This is because a velocity-based assessment framework is considered to be more meaningful for structures whose expected improved performance relies on the addition of velocity-dependent devices. The elastic threshold was set at velocity amplitudes around 0.9 m/s. Ground velocity amplitudes up to 0.5, 1.0, 1.5 m/s, and beyond were classified as small, moderate, strong, and severe earthquakes, respectively (Table 1). Strong levels of five ground motions that induced damage in the structures are displayed in Figure 2; there, alongside the plot of the accelerations, the input energy spectrum relative to each ground motion is also displayed. These spectra allow a comparison among the levels of input energy that is introduced to a single-degree-of-freedom system, with mass = 1 kN, inherent damping ratio (ζ) = 2%, and fundamental period T ranging between 0.1 and 7 s and subjected to different ground motions. In Figure 3, severe levels of other two ground motions that induced damage in the structure are displayed. Strong levels of these two records (Northridge and El Maule) did not cause damage to the structure. In Figure 4, severe level of the Michoacan earthquake is displayed. Note that this earthquake did not produce any damage to the structures at all. The damage threshold of the structures seems to be associated with the high levels of input energy introduced by the first period of vibration (Izmit-Kocaeli), by both the first and second periods (El Centro-270 and New Zealand), or by the second period alone (Kobe, El Centro-180, Northridge, and El Maule). These earthquake records were downloaded via the Strong-motion Virtual Data Center (CESMD).[22]

TABLE 1 Selected ground motions and factors chosen to scale them to the four earthquake levels used in this study

No.	Event/Station/Component	PGA (g)	PGV (m/s)	PGA/PGV	Factors to scale earthquakes to			
					Small	Moderate	Strong	Severe
1	Izmit-Kocaeli, Yarimca, 90	0.230	0.91	2.54	0.50	1.00	1.50	2.50
2	Michoacan, SCT1, N90W	0.158	0.57	2.76	0.80	1.60	2.50	4.00
3	El Centro, no.117, 270	0.210	0.37	5.69	1.25	2.50	4.00	6.70
4	El Maule, Concepcion, Long.	0.393	0.68	5.81	0.70	1.40	2.20	3.60
5	Northridge, Newhall–County Fire, 90	0.580	0.75	7.75	0.65	1.25	2.00	3.30
6	New Zealand, Greendale, N55W	0.738	0.95	7.81	0.50	1.00	1.50	2.50
7	Kobe, KJMA, 90	0.600	0.74	8.07	0.65	1.25	2.00	3.30
8	El Centro, no.117, 180	0.342	0.33	10.22	1.40	2.80	4.40	7.00

Note. PGA: peak ground acceleration; PGV: peak ground velocity.

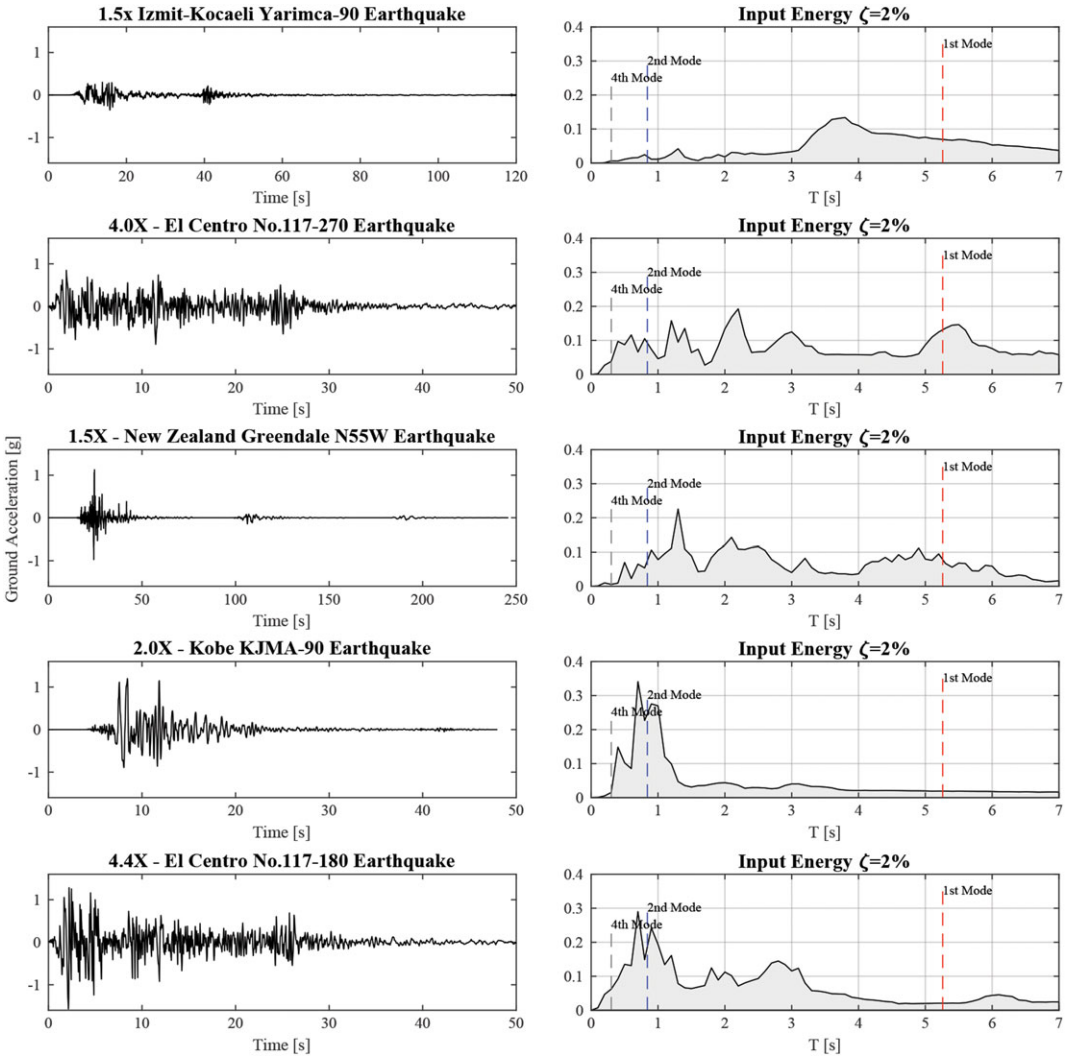

FIGURE 2 Five (out of eight) scaled ground motion records used in this study. Displayed accelerations, corresponding to strong earthquake level, caused damage to the single damped outrigger structure

3 | OPTIMAL DAMPING RATIO (*Z*) UNDER FEE VIBRATION

All the optimal inherent damping ratios described hereafter are in absolute values, that is, the original damping ratio = 2% is included in these optimal ratios. Hence, an optimized ζ = 8% represents a gain of 6% in damping.

3.1 | Single damped outrigger

Optimized ζ = 8% is obtained when the single damped outrigger is at λ = 0.7–0.8 and C_d = 9.60E + 04 kN-s/m (Figure 5).

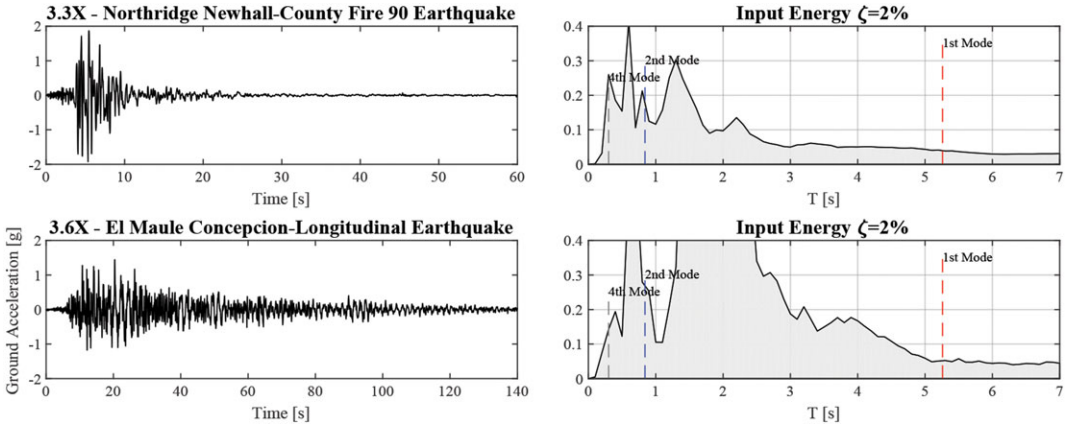

FIGURE 3 Two (out of eight) scaled ground motion records used in this study. Displayed accelerations, corresponding to severe earthquake level, caused damage to the single damped outrigger structure

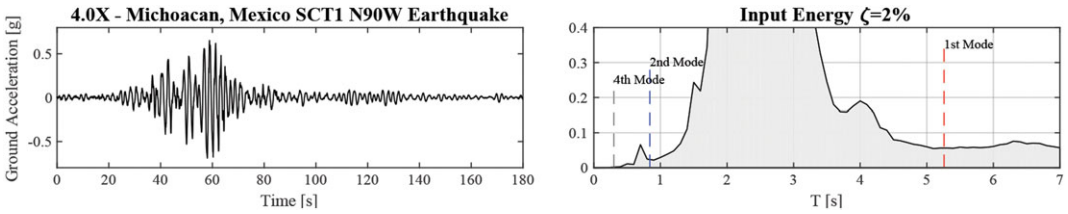

FIGURE 4 One of the eight scaled ground motion record used in this study. Displayed accelerations, corresponding to severe earthquake level, did not cause damage to any of the outrigger structures

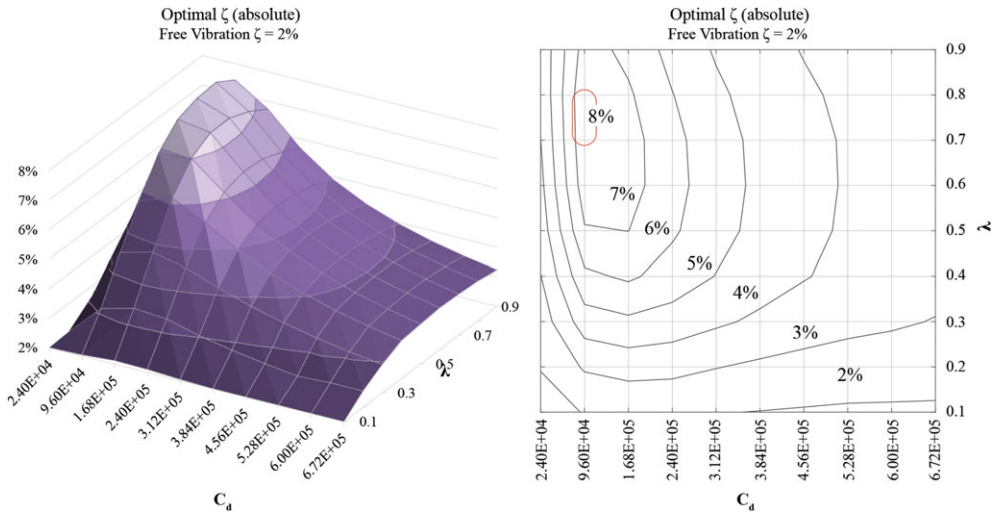

FIGURE 5 Optimal ζ in absolute values under a single damped outrigger configuration

3.2 | Double damped outriggers

Optimized ζ = 8.8% is obtained when the first set of damped outriggers (Outrigger 1) is at λ = 0.5 and the second one (Outrigger 2) at λ = 0.7–0.8 (Figure 6). The optimal C_d distribution at Outrigger 1 was first evaluated (although not showed here for the sake of brevity), resulting in a larger ζ obtained when C_d = 1.68E + 05 kN-s/m, and hence, this value is assumed optimal for the study of the C_d distribution at Outrigger 2. The optimized ζ = 8.8% is obtained when C_d values at Outrigger 2 are 3.84E + 05 (C_d6) and 4.56E + 05 (C_d7) kN-s/m, for λ = 0.8 and 0.7, respectively. Because it is assumed that a lower C_d implies the use of either fewer or more economical devices, the optimal double damped outriggers structure attaches the second set of outriggers at λ = 0.8.

3.3 | Double fixed outriggers

Compared with ζ = 2% given by the cantilevered core wall, the use of two sets of fixed outriggers is decreasing the damping to 1.4–1.8%, depending on the combination of outriggers' locations (Figure 7). In this context, the optimized ζ = 1.8% is obtained when the first set of fixed outriggers

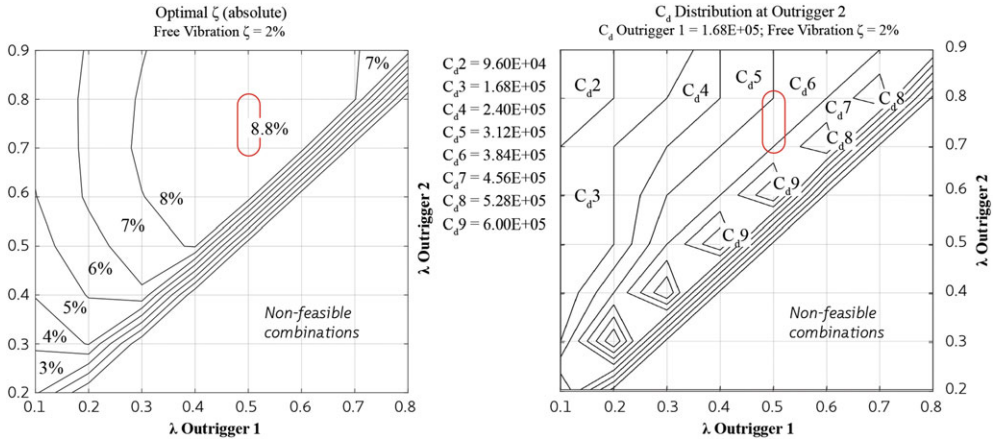

FIGURE 6 Optimal ζ (absolute values) under a double damped outrigger configuration (C_d outrigger 1 = 1.68E + 05 kN-s/m) and C_d distribution at Outrigger 2 according to optimal λ combinations

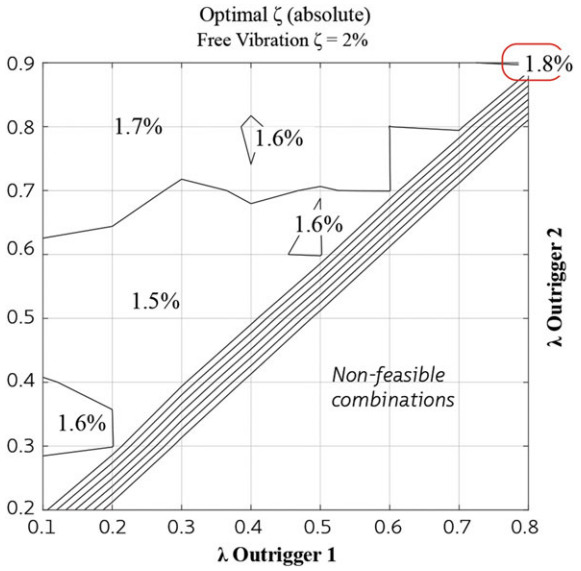

FIGURE 7 Optimal ζ (absolute values) under a double fixed outrigger configuration

(Outrigger 1) is at λ = 0.8 and the second one (Outrigger 2) at λ = 0.9. The result shows that the optimum positions for the two fixed outriggers are very close to each other. This basically indicates that a single fixed outrigger would be enough and possibly more economical than implementing two fixed outriggers in the structure.

3.4 | Combined damped and fixed outriggers

Optimized ζ = 8.6% is obtained when the lower set of damped outriggers is at λ_1 = 0.5 and the second set of fixed outriggers is at λ_2 = 0.7 (Figure 8). C_d of the dampers attached to Outrigger 1 is 1.68E + 05 kN-s/m.

3.5 | Combined fixed and damped outriggers

Optimized ζ = 6.2% is obtained when the lower set of fixed outriggers is at λ_1 = 0.1 and the second set of damped outriggers is at λ_2 = 0.7, which is slightly better than that at 0.6 (Figure 9). C_d of the dampers attached to Outrigger 2 is 9.60E + 04 kN-s/m. This result is comparable with Figure 5 in which the structure involves only one damped outrigger and hence, leading to the thought that the configuration of a fixed and a damped outrigger is not economical.

4 | ENERGY DISSIPATION UNDER STRONG EARTHQUAKES

Due to space constraints, only optimal configurations—based on increased ζ—were further studied. Hereafter, *single* damped, *double* damped, and *combined* damped and fixed outriggers refer to a single damped outrigger at λ = 0.7, to a set of double damped outriggers at λ = 0.5 and 0.8, and to a combined damped outrigger (λ = 0.5) plus a fixed outrigger (λ = 0.7), respectively.

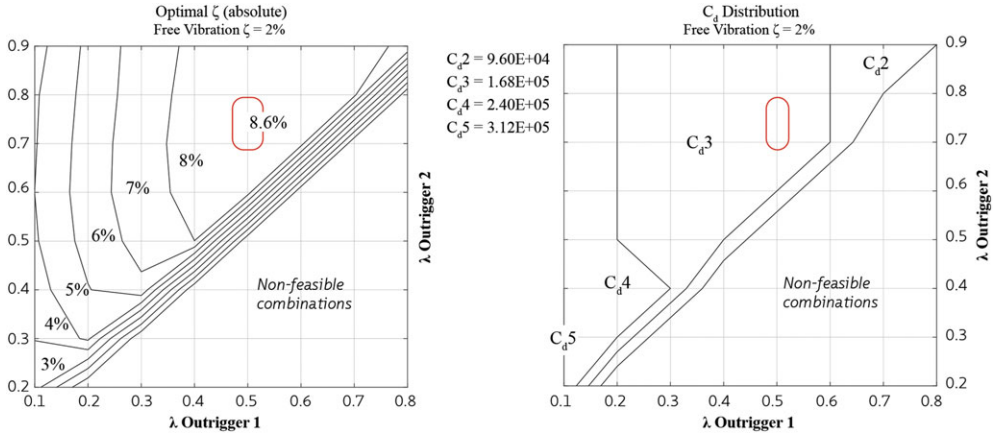

FIGURE 8 Optimal ζ (absolute values) under a combined damped (λ_1) and fixed outrigger (λ_2) configuration and C_d distribution according to optimal λ combinations

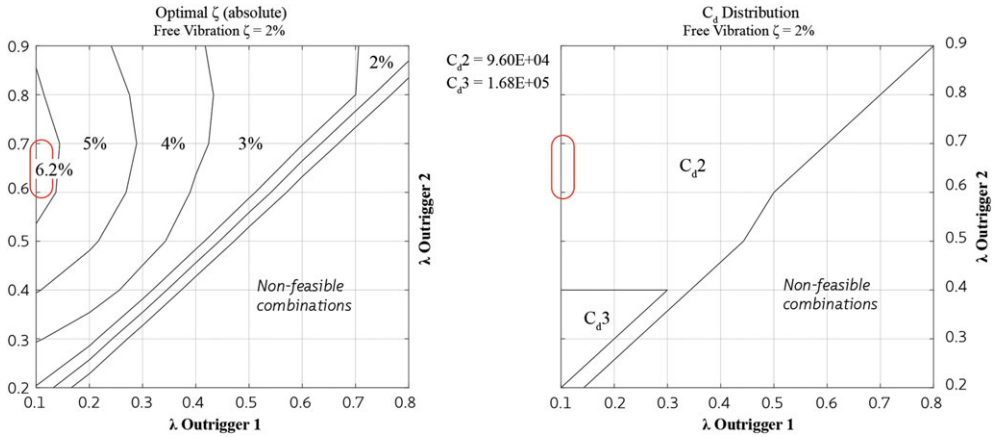

FIGURE 9 Optimal ζ (absolute values) under a combined fixed (λ_1) and damped outrigger (λ_2) configuration and C_d distribution according to optimal λ combinations

In order to generate a valid parameter for comparison, the scattered data produced by the energy-based assessment of the structures subjected to each earthquake record were fitted into a trend line using the function *polyfit* and *polyval* in Matlab.[23]

4.1 | Single damped outriggers

Despite the variations displayed by the individual plots—corresponding to each earthquake—the trend lines of E_D/E_I and $E_{dampers}/E_I$ are almost equal for the severe and strong levels of the selected ground motions (Figure 10). Hysteretic energy distribution presents, nevertheless, a small increase (from 0.14 to 0.19) under severe levels due to the additional non-linear performance of the structure under El Maule and Northridge earthquakes. Michoacan earthquake did not produce structural damage.

The reason why in average $E_D > E_{dampers}$ is related with the number and types of earthquake records selected for the study. For example, if only the records of Izmit-Kocaeli, Michoacan, and El Centro-270 had been considered, the figure would display a trend where $E_{dampers} > E_D$, by a large extent. If the records of El Centro-180, Kobe, and Northridge are considered, the plot would show again a trend $E_D > E_{dampers}$ but, this time, exhibiting a larger difference. The specific reason why under some earthquakes $E_D > E_{dampers}$ is because of their very low peak ground acceleration/peak ground velocity ratio (Table 1), which implies that the larger the velocity and the smaller the acceleration of an earthquake, the better the performance of the dampers. The only exception to this "rule" is the New Zealand record, whose influence seems to be rather associated with the "pulses-like" ground motion.

On the other hand, the reason why it takes longer for $E_{dampers}$ to reach a constant value seems to be associated with the fact that the source of E_D is the core. Whereas dissipation of energy by the core begins with the ground motion (at instant t = 1), the actions of dampers only begin when the building response has reached some rotation at the level of the damped outriggers, which occurs later on.

4.2 | Double damped outriggers

When increasing the ground motion from strong to severe levels (Figure 11), the use of a double set of damped outriggers does not present significant differences in the average energy dissipation due to structural damping (~45%), dampers (~40%), and hysteresis (~13%). However, if

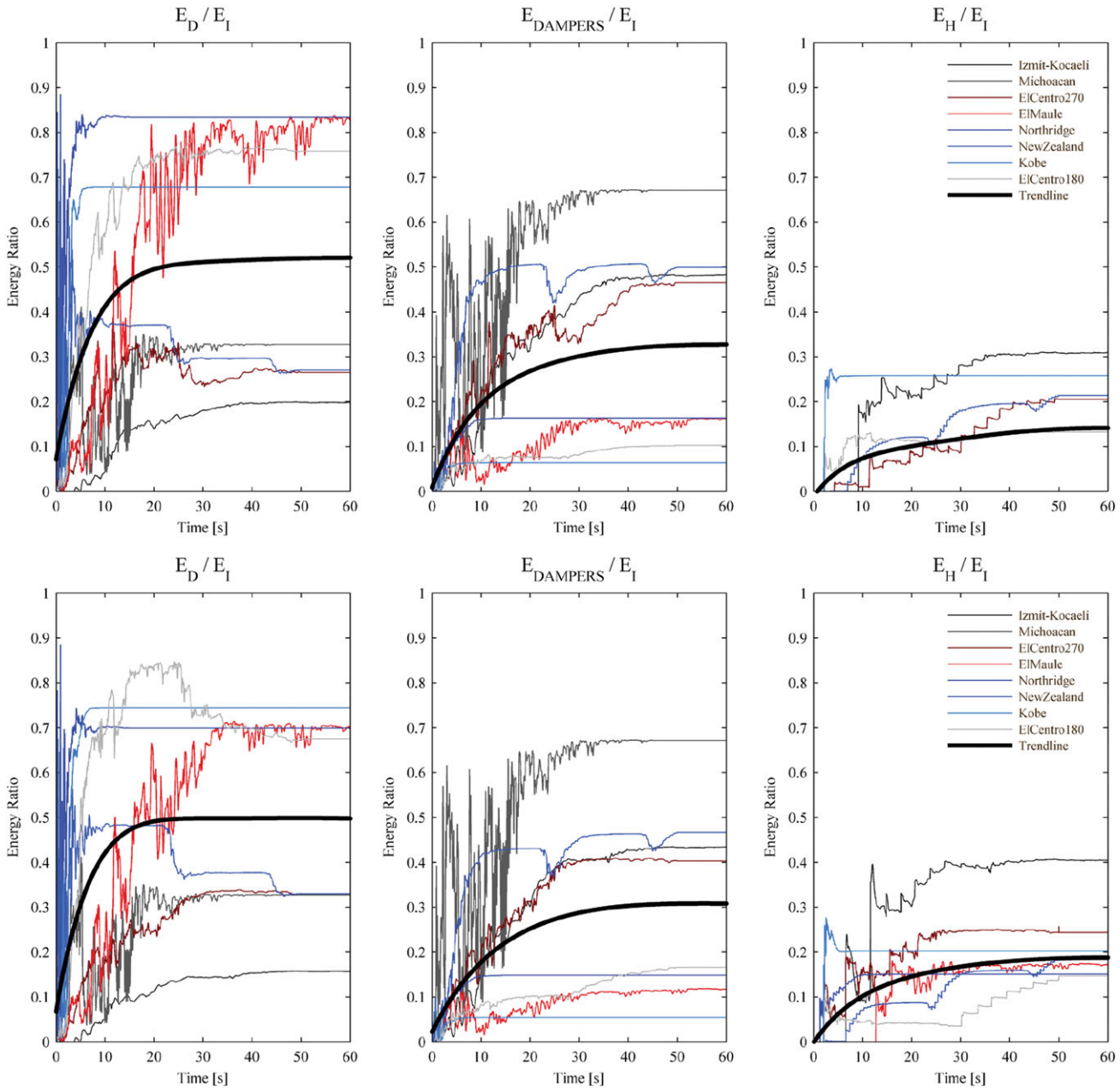

FIGURE 10 Energy dissipation ratios of the *single* damped outrigger under strong (upper row) and severe (lower row) levels of the selected eight earthquakes

compared with the average energy dissipated by the single damped outrigger, it can be noticed a decrease from 0.19 to 0.13 in the hysteretic energy dissipation and an increase from 0.30 to 0.40 in the dampers energy dissipation. Whereas the increase in the energy dissipated by the action of the viscous dampers may be explained by the extra number of dampers, the reduction in the average hysteretic energy is derived from the individual reduction in the hysteretic energy ratio of the structure under each earthquake. In this sense, notorious is the fact that under severe levels of El Maule and Northridge earthquakes, E_H/E_I is very small if compared with similar response of the single configuration. In simple words, under severe levels of certain earthquakes, the double damped outrigger reduces the damage to a minimum.

4.3 | Combined damped and fixed outriggers

In similar fashion with the previous two configurations, when the level of ground motions increases from strong to severe, the combined damped and fixed outriggers configuration does not present significant variations in the energy dissipation ratios (Figure 12). If compared with the single configuration, nevertheless, there is a reduction in the average energy dissipation due to hysteresis from 0.19 to 0.15, in the case of the severe level. As in the double damped case, this reduction can be attributed to the small contribution of the hysteretic energy of the structure when subjected to severe level of El Maule and Northridge earthquakes.

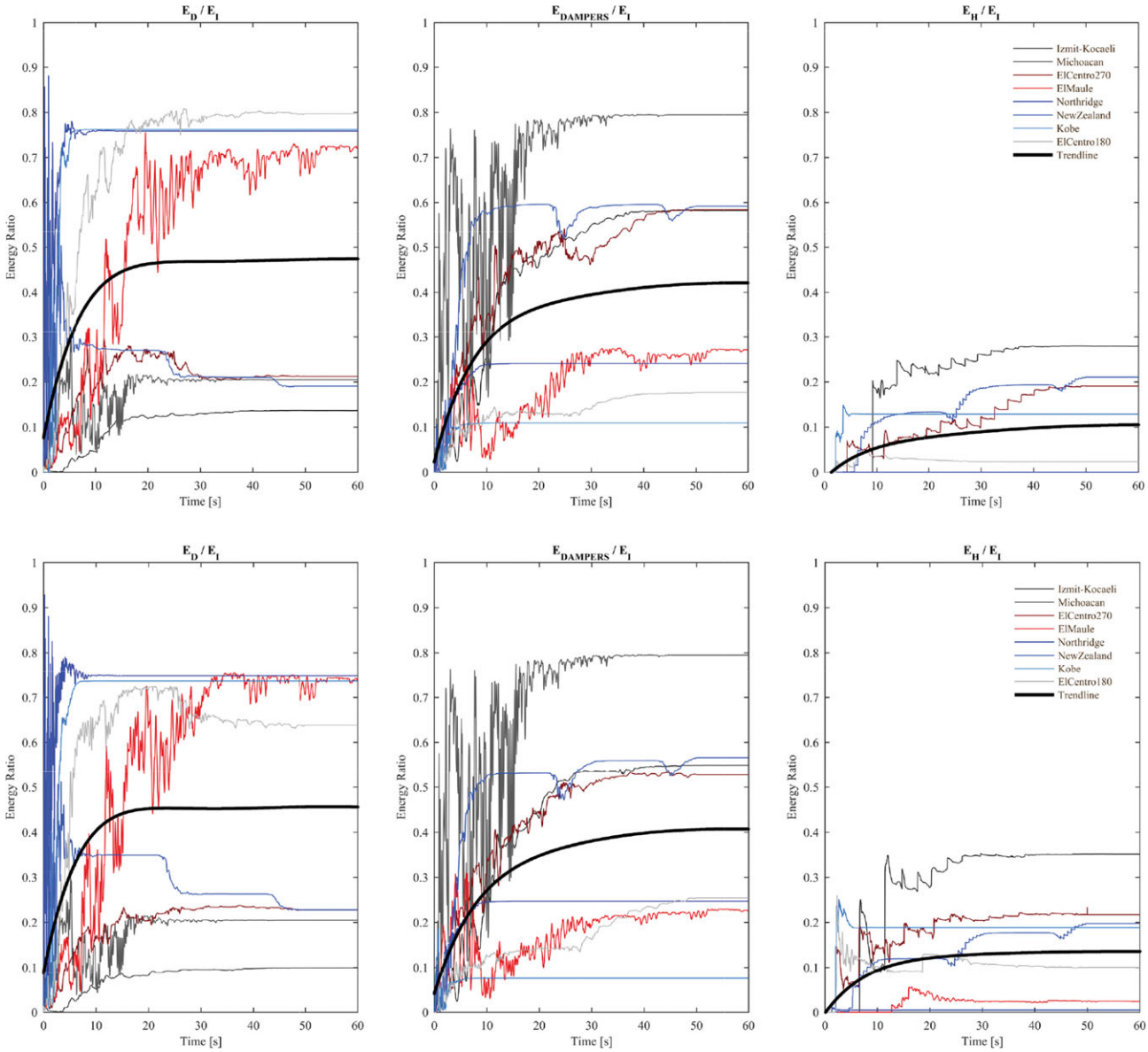

FIGURE 11 Energy dissipation ratios of the *double* damped outrigger under strong (upper row) and severe (lower row) levels of the selected eight earthquakes

5 | DECREASE IN STRUCTURAL RESPONSE

5.1 | Peak interstorey drift

The interstorey drift was normalized by the target drift = $h_s/555$, where h_s = storey height. Values larger than 1.0 are assumed to likely produce damage in the structure. The displayed trend line in Figure 13 is the average of the peak interstorey drift of the structures subjected to the four different earthquake levels. Despite small variations in the plots, there are no significant differences between *single*, *double*, and *combined* configurations in terms of reducing drifts. Moreover, the locations of these maxima values—except for two specific cases—are always among the five upper floors, that is, between the 55th and 60th floor. The two exceptions are the single and combined configurations, under the severe level of Michoacan earthquake, whose peak interstorey drifts occur at the 53rd and 54th floor, respectively.

5.2 | Peak accelerations

Despite some individual variations (e.g., severe level of Northridge case), the average peak accelerations remain fairly invariable for all the studied cases (Figure 14). Equally steady is the location of the peak acceleration at the building's roof, except for the strong and severe levels of Kobe earthquake, under which the peak acceleration takes place at the 32nd floor.

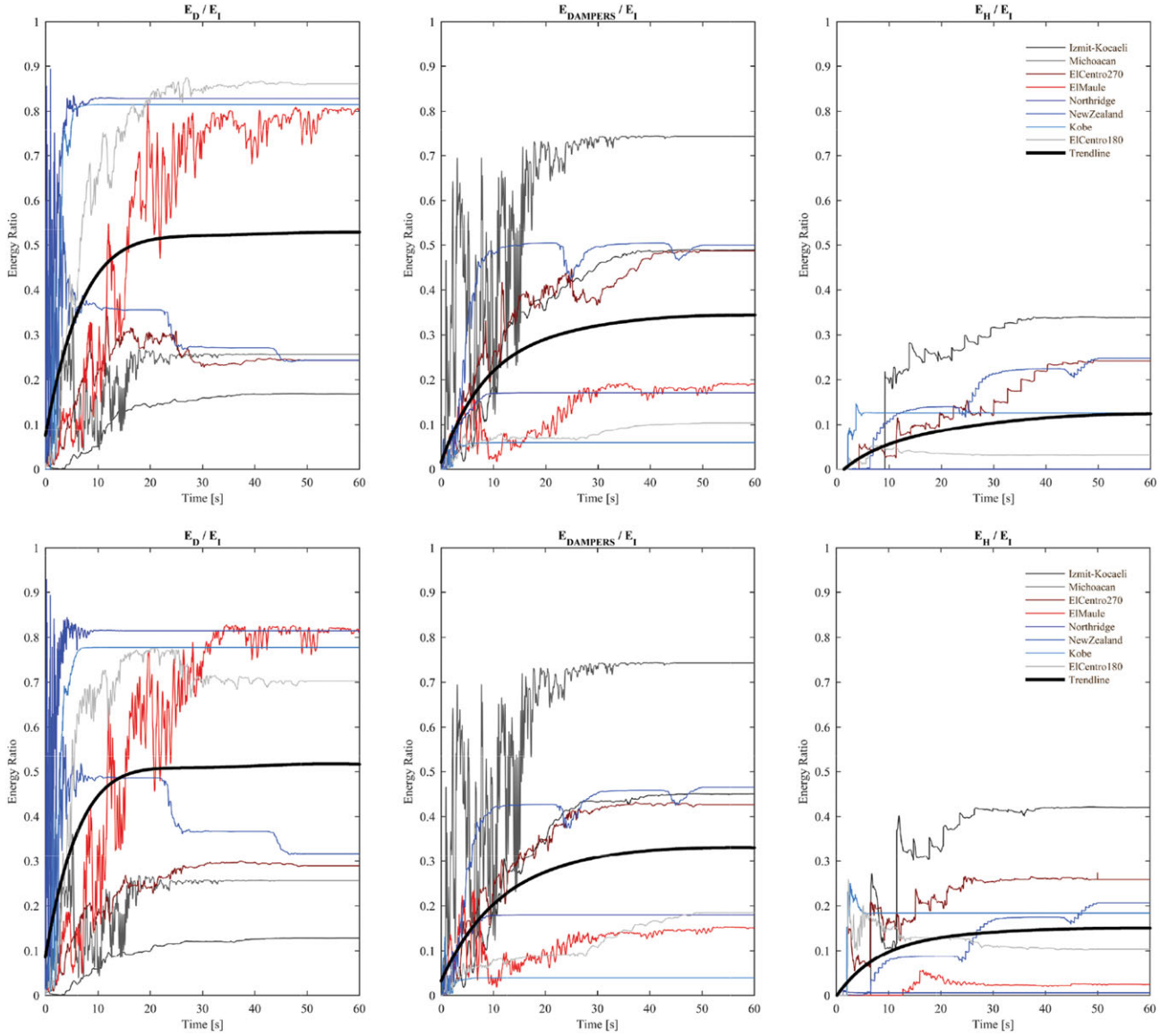

FIGURE 12 Energy dissipation ratios of the *combined* damped and fixed outrigger under strong (upper row) and severe (lower row) levels of the selected eight earthquakes

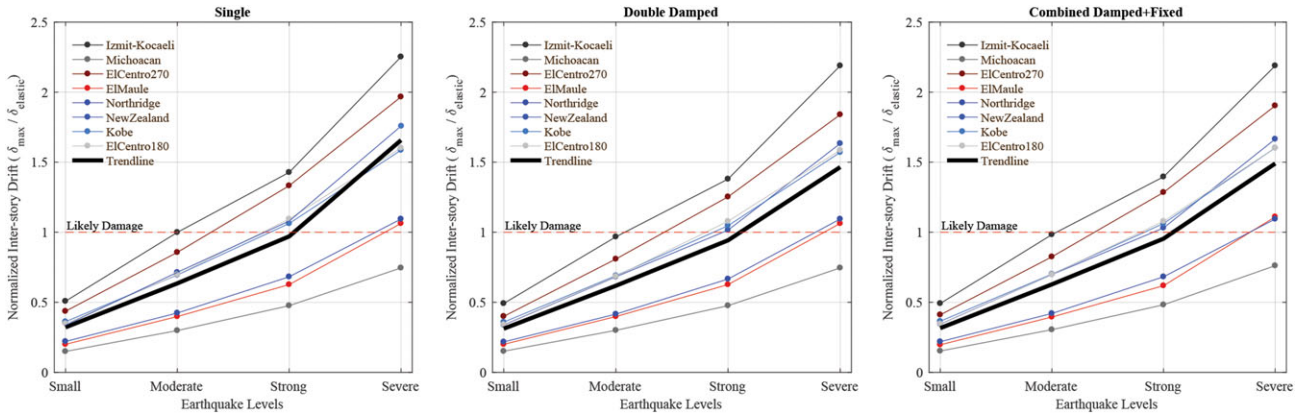

FIGURE 13 Normalized peak interstorey drifts of the studied outrigger configurations

5.3 | Peak base shear

The peak base shear plots resulting from the different configurations subjected to all levels of the selected ground motions are displayed in Figure 15. Peak base shear was normalized by the total seismic mass (W) of each configuration: 8.05E + 04, 8.10E + 04, and 8.08E + 04 tons

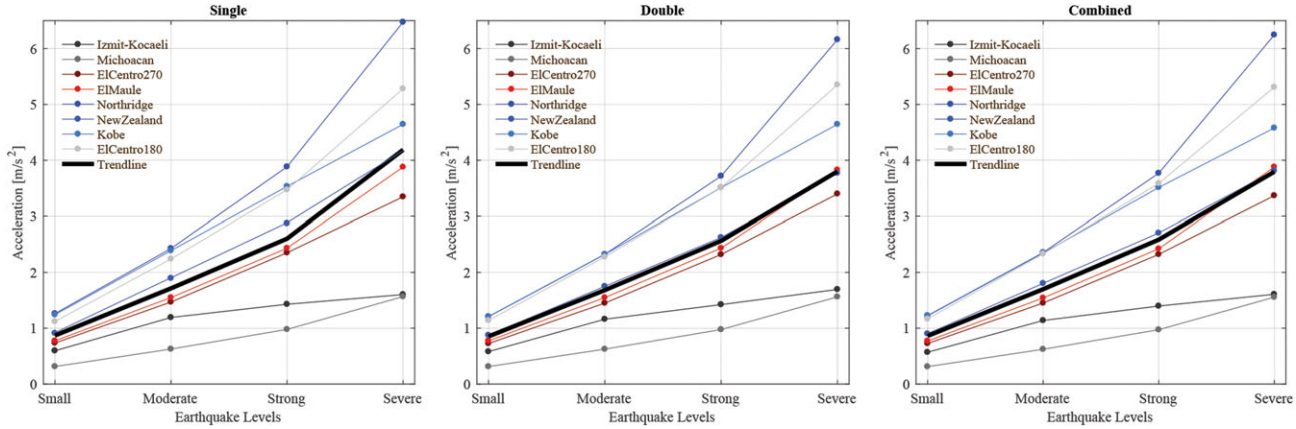

FIGURE 14 Peak accelerations (m/s^2) of the studied outrigger configurations

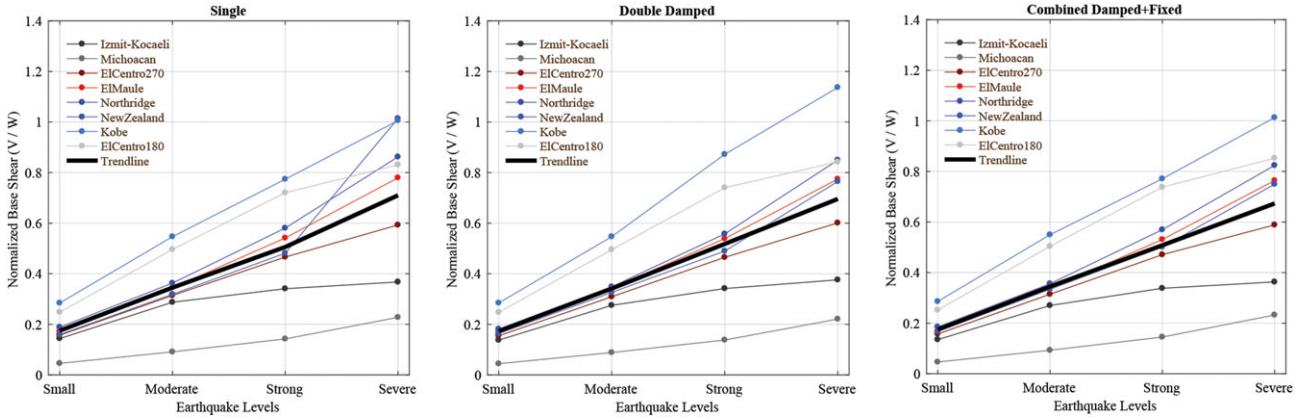

FIGURE 15 Normalized peak base shear (*V*/*W*) of the studied outrigger structures subjected to four earthquake levels of all ground motions

for single, double, and combined outriggers, respectively. Despite the individual variations, the trend lines in each plot of Figure 15 do not reveal substantial variation between the different configurations evaluated.

5.4 | Stresses and OTM

Although peaks of OTM and stresses might not occur at the same instant of the time-history of an earthquake, plots addressing the relationship between these peaks were elaborated to study their mutual influence in the non-linear structural response. Peak OTMs were normalized by the maximum OTM produced by a ground motion (Kobe earthquake in all cases); maximum stresses were normalized by the yielding stress; thus, $\sigma/\sigma_{yield} = 1$ represents the inelastic threshold. From the plots displayed in Figure 16, it can be noticed that (a) there is no substantial difference between the response trend lines (average) of each configuration, and (b) inelastic responses are triggered when peak OTMs are ~60% of the maximum OTM, for all the evaluated configurations.

In addition, all the non-linear responses induced in the single, double, and combined configurations by the strong and severe level of the selected earthquakes were provoked by the overpass of the core's tensile strength, that is, by yielding of the longitudinal reinforcement. As expected, all non-linearities—for all the cases—took place in the plastic hinge region of the core, that is, between the first and sixth floor.

Because all damage was induced in the core, the response of all outrigger frames—for all models—remained elastic, regardless of the level and the ground motion applied (Figure 17), indicating that no damage was produced in the outrigger. However, compared with the single damped outrigger, there is a clear decrease in the stress levels of the outrigger frame in both double and combined configurations. Because all the outrigger frames are modelled with I steel profiles, this decrease in the stress levels may convey cost-saving designs of double and combined configurations, due to the associated reduction in the required size of the steel profiles. Finally, when ratio $M_\theta/M_{\theta\text{-max}}$ is ~0.6 (inelastic threshold of the core), in the double configuration, there is a change in slope of the trend line, indicating that some of the stress is reduced due to the core's damage.

In the case of the perimeter columns (Figure 18), there is a substantial increase in the stress levels when two sets of damped outriggers are used. At the same time, there is no difference between stress levels of the columns between the single and combined configurations. This phenomenon can be explained by the dynamic stiffness provided by the addition of several viscous dampers in the double configuration, which increases the axial forces over the perimeter columns, whose sections remained the same for all configurations, and hence, axial stress levels are larger than those resulting from configurations where there is only one set of damped outriggers, that is, single and combined configurations.

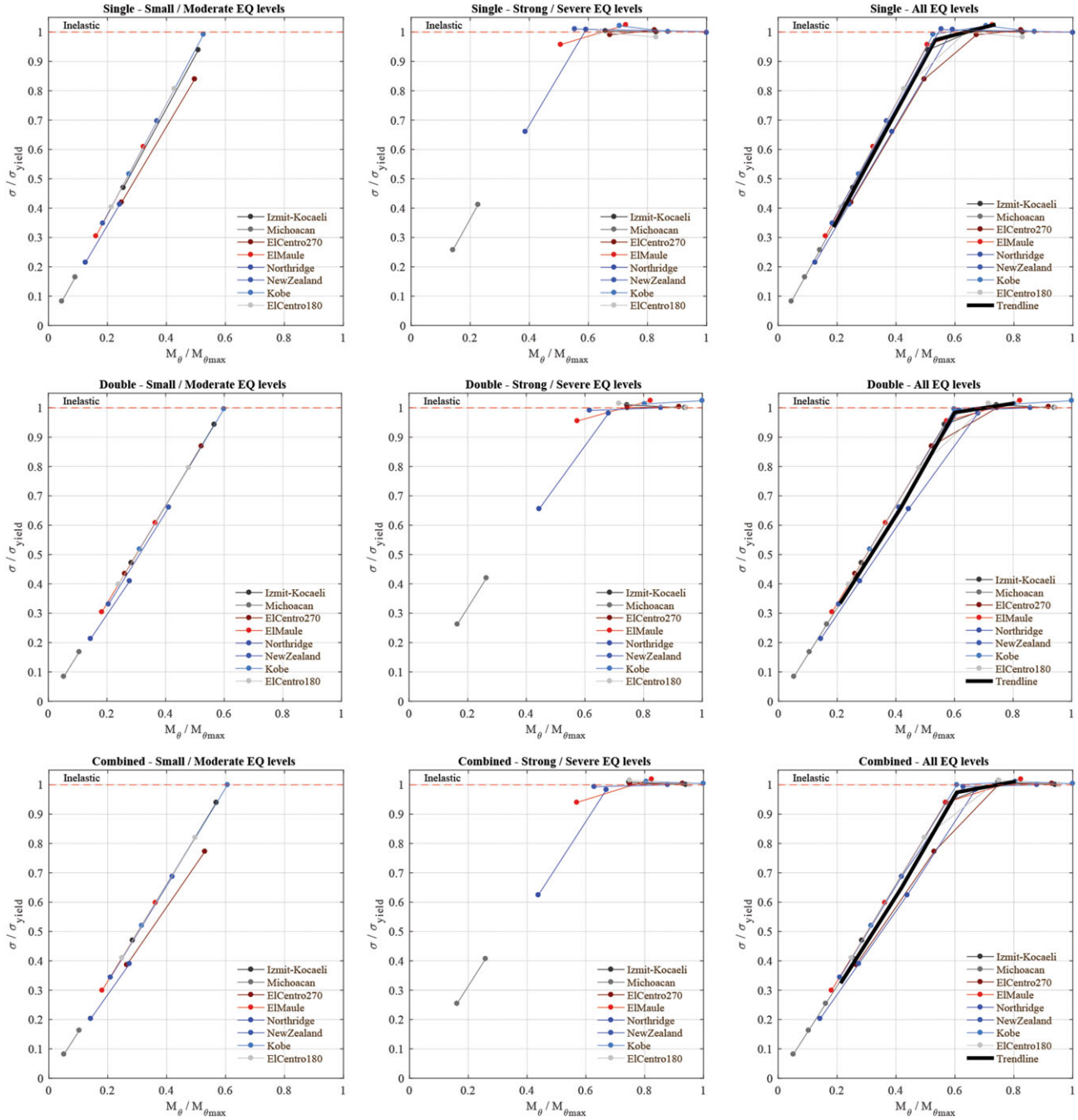

FIGURE 16 Normalized *core* stress (σ/σ_{yield}) to normalized overturning moment ($M_\theta/M_{\theta\text{-}max}$) of the single (upper row), double (middle row), and combined (lower row) outrigger configurations subjected to four earthquake levels of all ground motions

6 | SIMPLIFIED ECONOMIC EVALUATION

Practical relevance of the current work was studied by conducting a simple economic evaluation of the analytical models, which possess altered number of outriggers and viscous damper configurations. The alternative hypothesis was, using outriggers combined with oil viscous dampers causes a significant reduction in the amount of required reinforcement steel at the building core, which in turn will also cause a decrease in reinforcement steel costs. Nevertheless, the additional costs incurred through introduction of oil viscous dampers to the structural system must be addressed as well. Therefore, in this simplified approach, the current work solely considered the trade-off between the material costs of reinforcement steel at the building core against the costs of viscous dampers. Acknowledging such costs as the number of workers, the social security contributions and earthquake losses through life cycle of the building were not taken into account.

To determine the cost of reinforcement steel required in each alternative, first, the base shear and OTM envelopes were determined by modal analysis. The five predominant modes, equivalent to 90% of the seismic mass in horizontal direction (Table 2), were combined using square root of sum of squares method, in order to obtain the modal storey shear and OTM envelopes of each configuration (Figure 19). Second, the ratio (%) of reinforcement steel to the vertical and horizontal sections of the building core was calculated according to the capacity flexural strength design

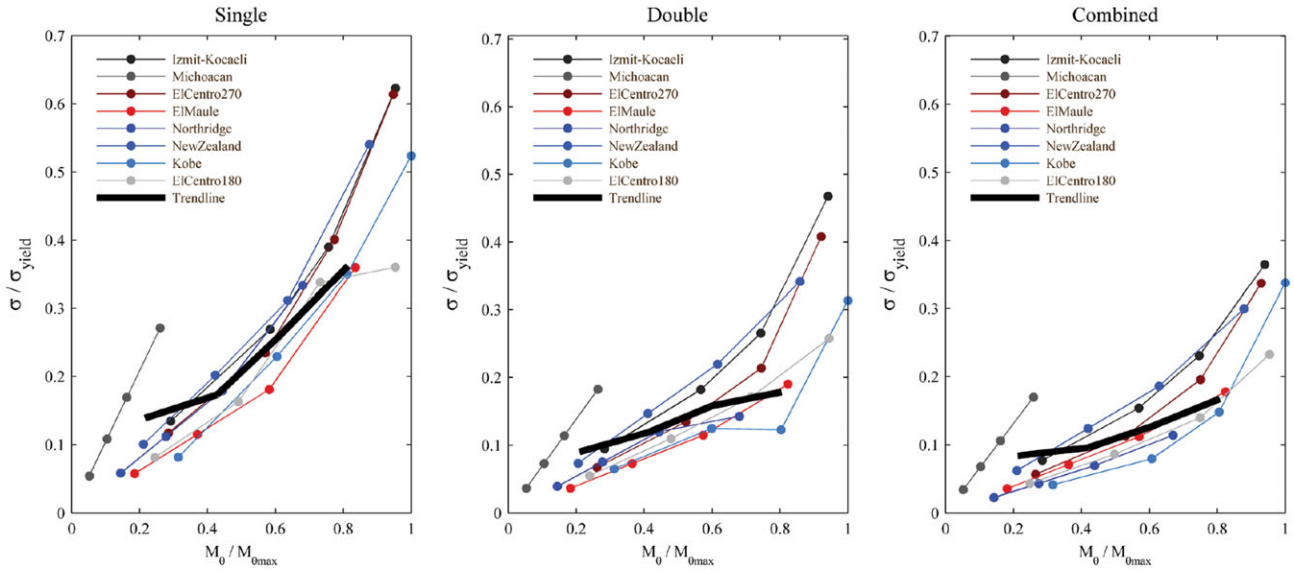

FIGURE 17 Normalized *outrigger* stress (σ/σ_{yield}) to normalized overturning moment ($M_\theta/M_{\theta\text{-}max}$) of the studied outrigger configurations subjected to four earthquake levels of all ground motions

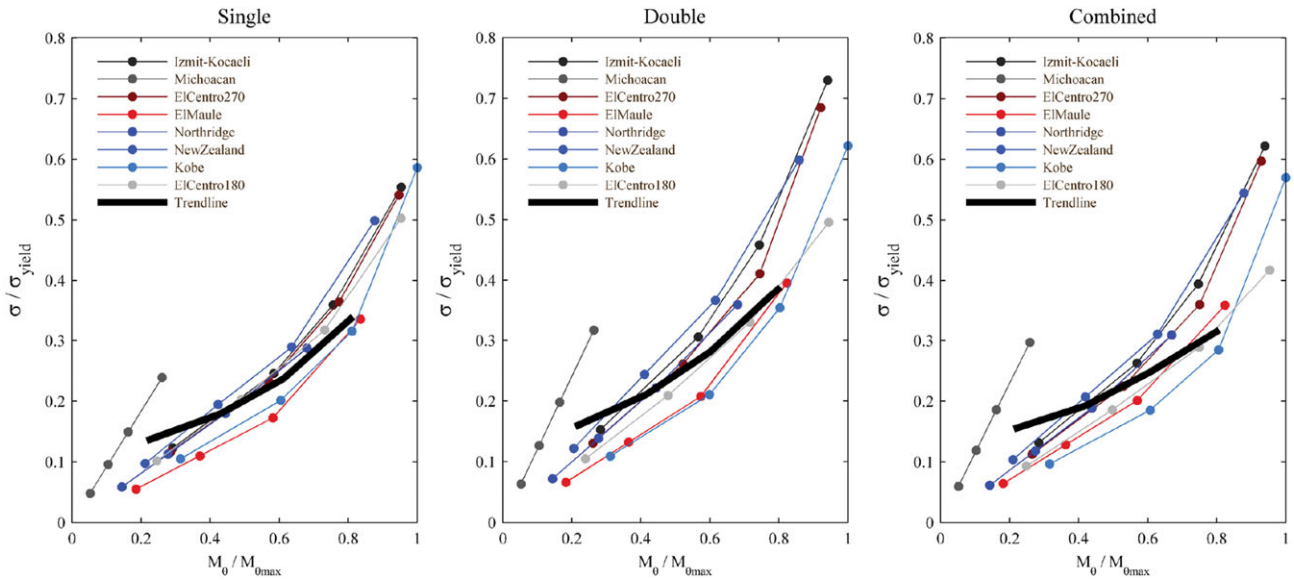

FIGURE 18 Normalized *column* stress (σ/σ_{yield}) to normalized overturning moment ($M_\theta/M_{\theta\text{-}max}$) of the studied outrigger configurations subjected to four earthquake levels of all ground motions

TABLE 2 Effective modal mass participation in X direction

Mode		1	2	4	5	7
T (s)	Single	5.26	0.84	0.30	0.17	0.16
	Double	5.27	0.85	0.31	0.20	0.16
	Combined	5.26	0.84	0.30	0.16	0.12
Effective mass-X (kN)	Single	4.98E + 04	1.51E + 04	5.02E + 03	1.99E-01	2.63E + 03
	Double	4.98E + 04	1.53E + 04	5.09E + 03	5.25E + 01	2.55E + 03
	Combined	4.97E + 04	1.53E + 04	5.07E + 03	2.57E + 03	1.75E − 02
Cumulative (%)	Single	62	80	86	86	90
	Double	62	80	87	87	90
	Combined	62	80	87	90	90

envelope, for a nonconservative case, as proposed by Boivin and Paultre.[17] In accordance with Eurocode,[16] the calculated vertical reinforcement ratios below the threshold level were replaced with the minimum reinforcement ratio requirement of 0.25%. Next, using these values and simple geometry, the total volume of reinforcement steel for each alternative was calculated. Multiplying these values with the density of the reinforcement steel provided the total weight in tons. In this work, market price of reinforcement steel per ton was assumed as $600.

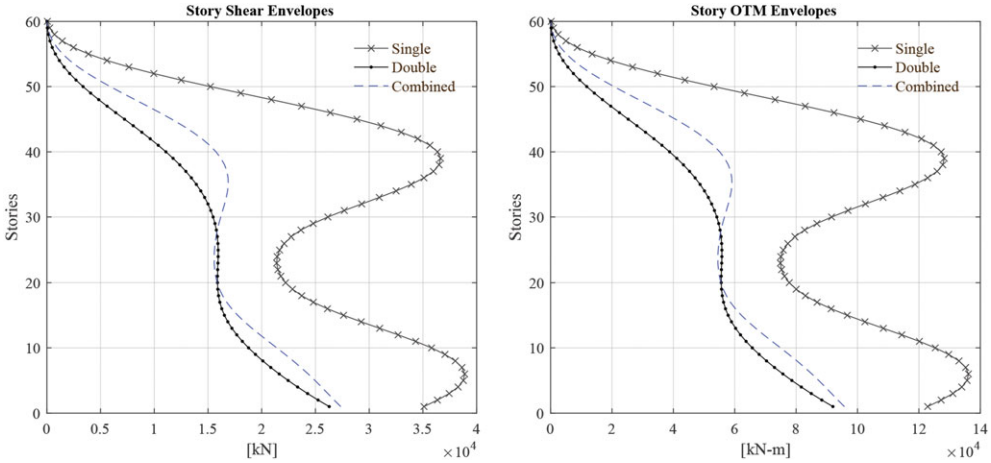

FIGURE 19 Square root of sum of square modal storey shear and overturning moment (OTM) envelopes for the three configurations of outriggers

Gidaris and Taflanidis[24] provided an empirical cost estimation model for oil viscous dampers based on maximum force capacity $F_{ud,j}$, as $\$96.88(F_{ud,j})^{0.607}$. In the current work, two different commercially available oil viscous damper types were used based on the required damping coefficient. Maximum force capacity of selected dampers is 2,000 kN, and therefore, the cost of one damper is estimated as \$9,771.46.

6.1 | Results of economic evaluation

The current work considered three alternatives of outriggers with oil viscous dampers. The calculated values are compared then to the results obtained from the alternative using conventional outriggers, called *conventional*, whose reinforcement demand was computed using a conservative approach. For each alternative, computed horizontal and vertical steel reinforcement values as required solely in the building core are outlined in Tables 3 and 4, respectively.

As previously defined, the terms *conventional*, *single*, *double*, and *combined* correspond to structural design alternatives that possess conventional outriggers, a single set of outriggers with dampers, two sets of outriggers with dampers, and two outriggers where one is fixed and one has dampers, respectively. In line with the provided definitions, the required number of dampers employed in *single*, *double*, and *combined* alternatives were computed as 8, 40, and 8, respectively (Table 5). These dampers are commercially available in seven sizes ranging from 1.25E + 04 to 8.75E + 04 kN. Hence, except for the case of the upper outrigger in the double alternative, one damper per outrigger is enough to provide the required supplemental damping. Two dampers were not yet enough for the upper outrigger in the double alternative (1.92E + 05/2 > 8.75E + 04, i.e., demand > supply); thus, four dampers were necessary to provide the required damping. Recall that, market price of reinforcement steel per ton was assumed as \$600, and the cost of one viscous damper was estimated as \$9,771.46. The results of comparative cost analysis among structural design alternatives considered in this work are given in Table 6.

The results suggest provision of the single outrigger system with dampers to the structural design of the hypothetical building core under the identical design loads caused 23% reduction in the reinforcement steel costs. The cost reduction became more significant at the level of 40% and 38% when double outrigger configurations were considered. Nevertheless, due to the high number of required dampers in the design alternative

TABLE 3 Required *horizontal* reinforcement steel values in the building core

	Required reinforcement steel ratios				Required reinforcement steel weight (kg)			
No. storey	Conventional	Single	Double	Combined	Conventional	Single	Double	Combined
1–6	0.50%	0.26%	0.19%	0.20%	44,510	22,699	16,994	17,686
7–12	0.44%	0.22%	0.17%	0.17%	39,168	19,862	14,870	15,476
13–18	0.37%	0.19%	0.14%	0.15%	32,937	17,025	12,746	13,265
19–24	0.31%	0.16%	0.12%	0.12%	27,596	14,188	10,621	11,054
25–30	0.25%	0.13%	0.10%	0.10%	22,255	11,350	8,497	8,843
31–36	0.25%	0.13%	0.10%	0.10%	22,255	11,350	8,497	8,843
37–42	0.25%	0.13%	0.10%	0.10%	22,255	11,350	8,497	8,843
43–48	0.25%	0.13%	0.10%	0.10%	22,255	11,350	8,497	8,843
49–54	0.25%	0.13%	0.10%	0.10%	22,255	11,350	8,497	8,843
55–60	0.25%	0.13%	0.10%	0.10%	22,255	11,350	8,497	8,843
Total weight (tons)					277.74	141.87	106.21	110.54

TABLE 4 Required *vertical* reinforcement steel values in the building core

	Required reinforcement steel ratios				Required reinforcement steel weight (kg)			
No. Storey	Conventional	Single	Double	Combined	Conventional	Single	Double	Combined
1–6	1.00%	0.93%	0.70%	0.73%	85,310	79,472	59,499	61,922
7–12	0.85%	0.84%	0.63%	0.65%	72,513	71,525	53,549	55,730
13–18	0.76%	0.75%	0.56%	0.58%	64,836	63,578	47,599	49,538
19–24	0.65%	0.65%	0.49%	0.51%	55,451	55,631	41,649	43,345
25–30	0.56%	0.56%	0.42%	0.44%	47,774	47,683	35,699	37,153
31–36	0.51%	0.41%	0.31%	0.32%	43,508	35,195	26,349	27,423
37–42	0.46%	0.32%	0.25%	0.25%	39,243	27,248	21,327	21,230
43–48	0.37%	0.25%	0.25%	0.25%	31,565	21,327	21,327	21,327
49–54	0.25%	0.25%	0.25%	0.25%	21,327	21,327	21,327	21,327
55–60	0.25%	0.25%	0.25%	0.25%	21,327	21,327	21,327	21,327
Total weight (tons)					482.85	444.31	349.65	360.32

TABLE 5 Supply of dampers according to the required damping coefficients (C_d′s)

Damping coefficient (kN)					No. dampers	
		Required at damping point[a]	Type	Supplied per damper	Per outrigger	Per set of outriggers
Single		4.80E + 04	B4	5.00E + 04	1	8
Double	Lower	8.40E + 04	B7	8.75E + 04	1	8
	Upper	1.92E + 05	B4	5.00E + 04	4	32
Combined		8.40E + 04	B7	8.75E + 04	1	8

[a]Equals to the optimal C_d divided by two, as two outriggers were modelled as one.

TABLE 6 Comparative cost analysis among structural design alternatives

Design alternative	Total reinforcement cost	Change compared with conventional model (%)	Cost of dampers	Total cost	Change compared with conventional model (%)
Conventional	$456,356	—	—	$456,356	—
Single	$351,712	−23%	$78,172	$429,883	−06%
Double	$273,521	−40%	$390,858	$664,380	+46%
Combined	$282,519	−38%	$78,172	$360,690	−21%

double, it is economically nonviable, as the total costs, defined as the sum of reinforcement steel cost and dampers cost, were 46% higher than the *conventional* design. One can deduce that high number of required dampers and their associated costs surpass the economic gains obtained from the reinforcement steel savings. *Single* and *combined* alternatives, on the other hand, presented an opposite figure. A relatively lower number of dampers required in the design of these alternatives kept the required dampers costs at the reasonable levels. Therefore, in these alternatives, the economic benefits obtained from reduction in the required reinforcement steel amount exceeded the economic losses caused by inclusion of dampers in the structural design. In particular, design alternative *combined* demonstrated a significant decrease in the total construction cost at the level of 21% when compared with *conventional* design and therefore proposed the most viable option, economically speaking. It should be noted, nonetheless, that the placement of the outrigger in the building was not considered in the cost analysis. Had it been so, the single outrigger structure might have presented advantages, from an economic perspective, over multiple outrigger structures.

7 | DISCUSSION

7.1 | Optimal configurations for increasing the inherent damping ratio ζ

In terms of ζ, only a double set of damped outriggers and the combined damped and fixed outriggers (attaching viscous dampers in the lower set of outriggers) displays larger increase than that of the single damped outrigger. Optimized ζ of the former two are 8.8% and 8.6%, respectively, which is in practical terms, almost the same but with the double damped outrigger requiring more dampers. Nevertheless, from an economical point of view, the use of combined damped and fixed outriggers is not only equally optimal but cheaper than its counterpart using a double set of damped outriggers.

In addition, it should be noticed that whereas a single damped outrigger exhibits optimal ζ only at λ = 0.7–0.8, both double and combined outrigger configurations exhibit broader display of optimal combinations (Figures 6 and 8), which offer flexibility of design to the high-rise architecture and distributions of building systems. It is worth to notice that the use of multiple outriggers is desired in tall buildings[3] and that their final locations depend on both the availability of space, say mechanical floors, and the influence of the outrigger members' size.[25]

7.2 | Optimal configurations for reducing the hysteretic energy

From the average ratios E_D, E_{dampers}, and E_H to E_I of the three studied configurations in Table 7, it is clear that both double damped and combined damped and fixed outriggers are reducing the hysteretic energy ratio (E_H/E_I) and hence becoming more effective in reducing structural damage under strong earthquake motions. However, as mentioned before, the double damped configuration requires the use of more dampers, and hence, it is assumed to be comparatively more expensive. The combined damped and fixed configuration, compared with the single damped one, is effectively reducing the hysteretic energy and maintaining the levels of energy dissipated by both inherent damping and viscous dampers.

Although a single set of conventional outriggers without dampers (*conventional*) was not included among the initial studied configurations, it was added for framing a valid performance bound. Thus, by observing the column E_H/E_I in Table 7, it can be noticed that the reduction in the hysteretic energy due to the addition of supplemental damping is not significant. For instance, no change and a decrease from 0.23 to 0.14 under strong and severe motion, respectively, are the results of comparing the cases of the conventional and double damped configurations. This relatively small decrease in E_H/E_I may be explained by two observations: (a) As indicated by a previous study of the authors,[14] the dampers' damping coefficient (C_d) and the outrigger's location (λ) are the parameters that most influence the tall building's response. Because these two parameters have been already optimized in each of the studied configurations, further improvements, beyond each optimal, are unlikely to take place; (b) as suggested by columns E_D/E_I and E_{dampers}/E_I, most of the energy dissipated by the dampers seems to be partially subtracted from that dissipated from the inherent structural damping.

Finally, the fact that the rows of energy dissipation ratios for the *single*, *double*, and *combined* configurations add up to 100% (column *Sum*, Table 7) indicates that these configurations are effective for reducing the building's response by the end of the ground motion. To the contrary, the *conventional* outrigger will continue vibrating beyond the end of the ground motion, and thus, part of the input energy will be dissipated as strain elastic energy.

7.3 | Optimal configurations for reducing the overall structural response

Interstorey drift can be reduced by adding outriggers, and it has been suggested that the effect of two sets of outriggers is, in this regard, better than one.[11] However, according to the results tabulated in Table 8, this is not necessarily the case when using damped outriggers. Whereas both double and combined outrigger solutions slightly reduce the maxima interstorey drifts when compared with the single configuration, the decrease is comparatively very small. This may be explained by the comparatively large influence of the outrigger location in the reduction of the interstorey drift; because there is no substantial difference in the location of the outriggers between both configurations, the interstorey drift is not affected largely. This seems to suggest that configurations with optimal ζ might not be further optimized for interstorey drifts reductions.

The almost non-existent variation among the peak acceleration response of all the configurations can also be explained by the difficulty of a further optimization after a damping ratio-based optimized design. Moreover, neither the addition of an extra set of outriggers nor viscous dampers will modify the seismic mass of the building substantially. Hence, there is no variation in the peak values of acceleration (Table 9). The fact that under the severe level of the Kobe ground motion, the system will experience its peak acceleration around half way of the height seems to indicate that—when subjected to this earthquake—the second mode shape has a larger influence in the response of the building. This

TABLE 7 Peak energy dissipation ratios (trend line-based), for each configuration under all earthquake levels

		E_D/E_I	E_{dampers}/E_I	E_H/E_I	Sum
Conventional	Small	0.93	—	0	0.93
	Moderate	0.93	—	0.01	0.94
	Strong	0.82	—	0.10	0.92
	Severe	0.72	—	0.23	0.95
Single	Small	0.61	0.39	0	1.00
	Moderate	0.61	0.39	0	1.00
	Strong	0.52	0.33	0.14	0.99
	Severe	0.50	0.31	0.19	1.00
Double	Small	0.52	0.48	0	1.00
	Moderate	0.52	0.48	0	1.00
	Strong	0.47	0.42	0.10	0.99
	Severe	0.45	0.41	0.14	1.00
Combined	Small	0.59	0.41	0	1.00
	Moderate	0.59	0.41	0	1.00
	Strong	0.53	0.34	0.12	0.99
	Severe	0.51	0.33	0.15	0.99

TABLE 8 Average normalized peak interstorey drifts

	Small	Moderate	Strong	Severe
Conventional	0.34	0.68	1.06	1.62
Single	0.32	0.64	0.97	1.50
Double	0.31	0.62	0.94	1.46
Combined	0.32	0.63	0.95	1.49

TABLE 9 Average peak accelerations (m/s^2)

	Small	Moderate	Strong	Severe
Conventional	0.88	1.74	2.60	3.84
Single	0.87	1.71	2.60	3.83
Double	0.85	1.68	2.56	3.80
Combined	0.86	1.70	2.59	3.79

observation is supported by the findings in Sun et al.[26] In their experimental study on seismic resonant behaviour of core-outrigger structure, the authors observed that large accelerations on the upper and middle floors resulted from the second-period resonant ground motion.

The same steady trend is observed in the results of normalized base shear in Table 10, wherein variations are fairly minimal. However, if the large variation of the average values for each earthquakes is considered (as displayed in Figures 13 and 15 for interstorey drifts and base shear, respectively), it seems that earthquake characteristics have a larger influence than outrigger configurations in the response of tall buildings.

From previous studies,[14] it is clear that under optimal design conditions, the addition of viscous dampers reduces both the OTM and overall stresses in the core, outriggers, and perimeter columns.

As it can be seen in Table 11, all damage produced by strong and severe earthquake levels, in the three studied configurations, is concentrated in the core. Due to the stress reduction in the outrigger's frame elements of the double and combined configurations, higher levels of axial stress appear in the perimeter columns. Moreover, by helping reduce the overall stress, the use of viscous dampers prevents the extension of damage as the ground motion grows larger, if compared with the response of the conventional outrigger. As mentioned before, inelastic responses are triggered when peak OTMs are ~60% of the maximum OTM, for all the evaluated configurations (Table 12).

As mentioned before, the fact that all the studied configurations have been optimized according to dampers' damping coefficient (C_d) and outrigger's location (λ), further improvements, beyond each optimal, are highly unlikely. This would explain the apparent uniformity in the response and the fact that from these results, it is not possible to conclude which configuration seems to be the optimal to reduce the overall structural response.

TABLE 10 Average normalized peak base shear

	Small	Moderate	Strong	Severe
Conventional	0.18	0.36	0.52	0.69
Single	0.17	0.35	0.50	0.68
Double	0.17	0.34	0.52	0.70
Combined	0.17	0.34	0.51	0.67

TABLE 11 Average normalized peak stresses

		Small	Moderate	Strong	Severe
Core	Conventional	0.37	0.74	1.02	1.00
	Single	0.34	0.68	0.97	1.00
	Double	0.33	0.66	0.98	1.02
	Combined	0.32	0.65	0.97	1.01
Outrigger	Conventional	0.14	0.24	0.33	0.55
	Single	0.14	0.17	0.26	0.36
	Double	0.09	0.12	0.16	0.18
	Combined	0.08	0.10	0.13	0.17
Column	Conventional	0.12	0.21	0.31	0.49
	Single	0.13	0.18	0.24	0.34
	Double	0.16	0.21	0.28	0.38
	Combined	0.15	0.19	0.25	0.32

TABLE 12 Average normalized peak overturning moment

	Small	Moderate	Strong	Severe
Conventional	0.23	0.46	0.64	0.83
Single	0.22	0.43	0.61	0.81
Double	0.21	0.42	0.60	0.80
Combined	0.21	0.42	0.61	0.81

8 | CONCLUSIONS

Although most of the conclusions obtained are only applicable to the specific cases described in this paper, general observations can be derived from the numerical studies presented herein:

- Among the studied outrigger configurations, only a double set of damped outriggers and the combined damped and fixed outriggers (attaching viscous dampers in the lower set of outriggers) display larger increase of ζ than the 8% of the single damped outrigger. Optimized ζ of the former two are 8.8% and 8.6%, respectively.
- A double set of outriggers including dampers only in the upper set will result in a lower damping ratio than that obtained with a damped outrigger alone. In simple words, attaching a conventional outrigger below the damped outrigger will decrease the structure's damping capability.
- Whereas a single damped outrigger exhibits optimal ζ only at λ = 0.7–0.8, both double and combined damped and fixed outriggers exhibit broader display of optimal combinations, which offer flexibility of design to the high-rise architecture and distributions of building systems.
- Both double damped and combined damped and fixed outriggers are reducing the hysteretic energy ratio (E_H/E_I). The double damped outrigger is more effective for reducing the damage in the structure when subjected to strong and severe earthquake levels.
- The fact that all the studied configurations have been already optimized according to dampers' damping coefficient (C_d) and outrigger's location (λ), further improvements, beyond each optimal, are highly unlikely to take place. This would explain the observed lack of major improvements in the response of double and combined damped and fixed outriggers compared with a single damped outrigger system.
- Given the C_d values involved in these optimal designs, and assuming the building costs mostly influenced by the amount of reinforcement steel and viscous dampers, the extra costs due to the double damped are about 50% more expensive than the single damped solution. To the contrary, the additional costs due to the combined damped and fixed solutions are about 16% cheaper than the single damped solution.
- It should be noted, nonetheless, that the placement of the outrigger in the building was not considered in the cost analysis. Had it been so, the single outrigger structure might have presented advantages, from an economic perspective, over multiple outrigger structures.

ACKNOWLEDGEMENTS

The authors thank the anonymous referees for their valuable comments and suggestions that helped to improve this paper. The first author's work in this research is supported by Fondo de Fomento al Desarrollo Científico y Tecnológico, through the project *BecasChile* (Grant 72100284). This support is gratefully acknowledged.

ORCID

Mauricio Morales-Beltran http://orcid.org/0000-0003-4883-4314

REFERENCES

[1] R. J. Smith, M. R. Willford, *Struct. Design Tall Spec. Build.* **2007**, *16*, 501.

[2] K. Park, D. Kim, D. Yang, D. Joung, I. Ha, S. Kim, *Int. J. Steel Struct.* **2010**, *10*, 317. https://doi.org/10.1007/BF03215840

[3] R. Smith, *Int. J. High-Rise Build.* **2016**, *5*, 63.

[4] M. Willford, R. Smith. Performance based seismic and wind engineering for 60 story twin towers in Manila. Proceedings of the 14th World Conference on Earthquake Engineering, (14WCEE), Beijing, China. **2008**.

[5] T. Asai, C.-M. Chang, B. M. Phillips, B. F. Spencer Jr., *Eng. Struct.* **2013**, *57*, 177.

[6] R. Gamaliel. Frequency-based response of damped outrigger systems for tall buildings, MSc. Thesis, Massachusetts Institute of Technology. **2008**.

[7] B. Huang, T. Takeuchi, *Earthq. Spectra* **2017**, *33*, 665. https://doi.org/10.1193/051816EQS082M

[8] Z. Wang, C.-M. Chang, B. F. Spencer Jr, Z. Chen. Controllable outrigger damping system for high rise building with MR dampers. Proc. SPIE 7647, Sensors and Smart Structures Technologies for Civil, Mechanical, and Aerospace Systems, 76473Z. **2010**.

[9] K. Deng, P. Pan, A. Lam, Y. Xue, *Struct. Design Tall Spec. Build.* **2014**, *23*(15), 1158.

[10] P. Tan, C. Fang, F. Zhou, *Earthq. Eng. Eng. Vib.* **2014**, *13*, 293.

[11] Y. Zhou, H. Li, *Struct. Design Tall Spec. Build.* **2014**, *23*(13), 963.

[12] P. Khashaee, B. Mohraz, F. Sadek, H. Lew, J. L. Gross. Distribution of earthquake input energy in structures. U.S. Department of Commerce. **2003**.

[13] C.-M. Uang, V. V. Bertero, *Earthq. Eng. Struct. Dyn.* **1990**, *19*, 77.

[14] M. Morales-Beltran, G. Turan, U. Yildirim, J. Paul, *Struct. Design Tall Spec. Build.* **2018**, *27*, e1463. https://doi.org/10.1002/tal.1463

[15] DIANA FEA Release 10.1 TNO - DIANA FEA BV Delft, the Netherlands. **2016**.

[16] 1992-1-1, E. Eurocode 2: Design of concrete structures - Part 1–1: General rules and rules for buildings. **2004**.

[17] Y. Boivin, P. Paultre, *Can. J. Civ. Eng.* **2012**, *39*, 738.

[18] Applied Technology Council (ATC 72–1), **2010**. Modeling and acceptance criteria for seismic design and analysis of tall buildings, Report No. PEER/ATC-72-1, CA, (p. 242).

[19] 1993-1-1, E. Eurocode 3: Design of steel structures - Part 1–1: General rules and rules for buildings. **2004**.

[20] E. Bojórquez, A. Reyes-Salazar, A. Terán-Gilmore, S. Ruiz, *Steel Compos. Struct.* **2010**, *10*, 331.

[21] M. Morales-Beltran. Smart energy dissipation: damped outriggers for tall buildings under strong earthquakes, Doctoral dissertation, Delft University of Technology. **2018**.

[22] CESMD, Strong-motion Virtual Data Center. **2014**. (Accessed Sep-2014 ww.strongmotioncenter.org)

[23] MATLAB. The MathWorks, Inc. Natick, Massachusetts, United States. **2013**.

[24] I. Gidaris, A. A. Taflanidis, *Bull. Earthq. Eng.* **2015**, *13*, 1003.

[25] H. S. Choi, L. Joseph, *Int. J. High-Rise Build.* **2012**, *1*, 237.

[26] F. Sun, Z. Hu, G. Chen, L. Xie, L. Sheng, *Struct. Design Tall Spec. Build.* **2017**, *26*, 1. https://doi.org/10.1002/tal.1349

AUTHOR BIOGRAPHIES

Mauricio Morales-Beltran is an architect and a structural engineer. He is a senior lecturer at the Faculty of Architecture, Yaşar University, Izmir, Turkey, and a PhD at the Faculty of Architecture and the Built Environment at Delft University of Technology, the Netherlands.

Gürsoy Turan is an assistant professor at the İzmir Institute of Technology–Department of Civil Engineering, BSc (Middle East Technical University), MSc, and PhD (University of Illinois at Urbana-Champaign). His research interests are structural dynamics and active control and structural analysis

Onur Dursun is an assistant professor at the Faculty of Architecture, Yasar University, Izmir, Turkey; Bachelor of Science in civil engineering from Istanbul Technical University (ITU) in 2006; Master programs at ITU and University of Reading, 2009; Dr-Ing at the Institute for Construction Economics, University of Stuttgart, Germany, 2014. His research interests are stochastic parametric modelling at the preplanning stages of building projects, building surrogate modelling in energy consumption and daylighting, and multiobjective evolutionary algorithms applied in architectural design.

Rob Nijsse is a professor of Structural Design–Department of Architectural Engineering + Technology at the Faculty of Architecture and the Built Environment. He is also director and senior constructions advisor at ABT. He has collaborated in the construction of the new building for Rabobank in Utrecht; high-rise office building in Seoul; the 100% glass bridge in Rotterdam linking two office blocks; the pavilion for the Sonsbeek sculpture exhibition; the University Library in Doha, Qatar (OMA); the multidisciplinary Taipei Theatre, Taiwan (arch. OMA); and a glass brick facade for a shop in Amsterdam's P.C. Hooftstraat (MVRDV).

How to cite this article: Morales-Beltran M, Turan G, Dursun O, Nijsse R. Energy dissipation and performance assessment of double damped outriggers in tall buildings under strong earthquakes. *Struct Design Tall Spec Build*. 2019;28:e1554. https://doi.org/10.1002/tal.1554